Contributions from parallel strategies for spatial orientation in *C. elegans*

Brian A. Dahlberg[1] and Eduardo J. Izquierdo[1,2]

[1]Cognitive Science Program, Indiana University Bloomington
[2]Luddy School of Informatics, Computing, and Engineering, Indiana University Bloomington
Corresponding email: bdahlber@iu.edu

Abstract

Understanding how brains and environments give rise to behavior is a subject of great multidisciplinary interest. *C. elegans* is well-suited for this work because of its relatively rich behavioral repertoire and tractable connectome. The chemotaxis of *C. elegans* is comprised of two complimentary strategies - "weathervane" (klinotaxis) and "pirouette" (klinokinesis) - that operate in parallel with one another. The present work seeks to characterize each strategy and its contribution to the overall chemotaxis behavior. We find that the contribution of klinotaxis is the primary contributor of chemotaxis performance in most environments, but that klinokinesis is effective in environments with faint stimuli, have few gradient sources or are noisy, particularly when it is integrating sensed concentration over a longer time-scale.

Introduction

Spatial orientation is a fundamental behavior for all living organisms. A particularly well-studied example of spatial orientation is chemotaxis, in which an organism senses a chemical concentration gradient and navigates either towards or away form its source. *C. elegans* is suited for this work because of its rich behavioral repertoire and tractable connectome (White et al., 1986; Sengupta and Samuel, 2009; Varshney et al., 2011; Izquierdo, 2019). Understanding the behavior well is a crucial building block towards this work. There are several spatial orientation behaviors that *C. elegans* exhibits, but a particularly well-studied one is chemotaxis. Chemotaxis behavior in *C. elegans* is comprised of two strategies that operate in parallel (Iino and Yoshida, 2009). The first strategy, klinokinesis, involves the organism modulating the chance that it performs a random reorientation. This strategy is also referred to as the 'pirouette' strategy in the literature. In the context of an attractive chemical, a reorientation is more likely to occur when the organism is traveling down the concentration gradient (i.e., away from the source), and less likely to occur when it is traveling up the gradient (i.e., towards the source). The second strategy, klinotaxis, entails the organism sensing the gradient during its dorsoventral head swings, effectively sampling the gradient perpendicular to its translational direction of movement, and gradually curving towards the direction with the highest concentration. This strategy is also referred to as the 'weathervane' strategy in the literature. These strategies are not only used to navigate in relation to chemical gradients in the environments, but they are also used for navigation in relation to odorants (White et al., 2007), temperatures (Gray et al., 2004), and oxygen (Bretscher et al., 2011). These strategies for spatial orientation are also not unique to *C. elegans*: for example, neutrophils employ a klinokinesis strategy to navigate towards wounded or infected tissue (Oliveira et al., 2017), while *Drosophilia* larvae employ klinotaxis to climb odor gradients (Gomez-Marin and Louis, 2014).

The goal of this paper is to better understand the contribution of each of these strategies to the overall spatial orientation behavior – especially how these contributions vary depending on the environment. Iino and Yoshida (2009) developed a computational model of the two strategies and reported on their contribution to chemotaxis in radial and grid chemotaxis assays. We have adopted their model in the present work and extended it with several environmental manipulations and a non-instantaneous pirouette model. Appleby (2014) used a neuron-level computational model to examine how the contribution from each of the strategies varies in different environment. However, a similar analysis in environments that resemble those of *C. elegans* more closely has not yet been done: the real environments are dynamic and often have multiple attractant sources. Thus, we build upon their work by proposing three significant extensions. First, in order to better understand the contributions of each strategy in different types of environments, we extend their work by considering environmental conditions where the number of NaCl point-sources ("spots" hereafter) vary. Second, we propose several more measures of chemotaxis performance that probe different aspects of performance, which will allow for a more fine-grained analysis of the contribution of the strategies. Third, following Iino and Yoshida (2009), we model the chemical concentration gradient after real-world NaCl diffusion. An important distinction that follows is that our gradient is dynamic, because it continues to

diffuse over the course of the simulated assays. We also replicate the parameters of chemotaxis assays, such as spot locations and amounts, model worm starting position, and duration of the assay.

We have embraced a computational modeling approach for several reasons. Most importantly, we are able to selectively enable and disable each strategy. With a computational approach we are also afforded precise control over our environments, and even able to make manipulations that would not be possible in the real world. We are also able to collect more fine-grained measurements of the worm's chemotaxis than we would be able to in an empirical setting, as well as run an otherwise impossible number of (simulated) assays.

Model

Following earlier work (Iino and Yoshida, 2009), we consider the organism as a point-agent navigating a two-dimensional environment containing a simulated NaCl concentration gradient. For the simulation, we renewed the position and direction of movement of a model worm every 0.1 seconds. The velocity of the model worm was set to a constant value of 0.12 mm/s, which is the average velocity of wild-type animals on chemotaxis plates. The heading of the model worm is modified by changes in the stimulus from the environment in two ways: klinokinesis and klinotaxis.

In the absence of a chemical gradient, worms have a natural curving bias that changes over the course of a run in a seemingly-random pattern and a baseline pirouette frequency (Iino and Yoshida, 2009). We incorporate both of these assumptions into our model worms. First, to instantiate the curving bias, at each step of the simulation, the heading of the worm is modified by Δh_b, which changes over time. Every 12 seconds a curving bias is drawn from a normal distribution (SD=32.3 °/mm). Over those 12 seconds, Δh_b linearly changes towards the random curving influence's value, and when it reaches it after 12 seconds, a new value is drawn again. Second, to instantiate the baseline pirouette frequency, there is a 0.0197 chance every second that the orientation of the worm will change to a new random one.

Klinokinesis

Klinokinesis operates by assessing the change in the sensed concentration over a period of time (Pierce-Shimomura et al., 1999). If the sensed concentration is decreasing, a random reorientation (or a pirouette) is likely to occur. If the concentration sensed is increasing, the likelihood of a piroeutte is suppressed. The sensorimotor transformation that determines the klinokinesis strategy is given by the probability of a pirouette (p) given the change in concentration (dC) over a window of time (dt) (Fig. 1A):

$$p = \frac{0.023}{\left(0.40 + e^{140\mathrm{d}C/\mathrm{d}T}\right)} + 0.0033 \qquad (1)$$

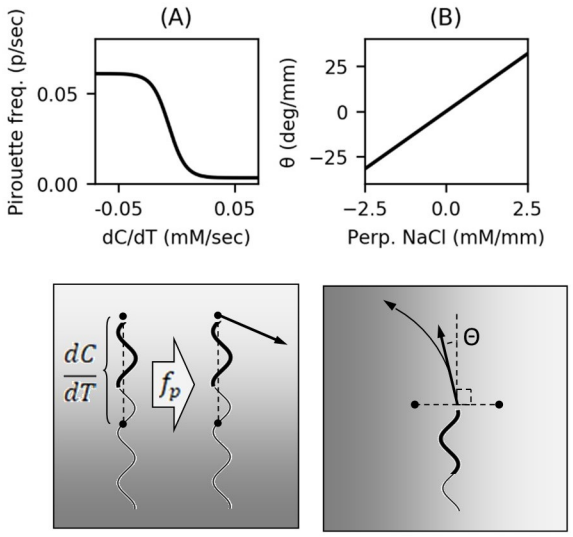

Figure 1: Sensorimotor transformations for the two orientation strategies. (A) During klinokinesis, model worms compare concentration over time across their translational direction of movement and modulate their pirouette frequency according to the magnitude of the change. (B) During klinotaxis, model worms compare the concentrations at the dorsal and ventral points perpendicular to their translational direction of movement and modulate their orientation gradually in the direction of higher concentration.

This strategy receives the most information about the gradient when the worm is heading directly towards or away from the gradient source.

Klinotaxis

Klinotaxis operates by assessing the gradient perpendicular to the model worm's translational heading, and gradually curving in the direction of greater concentration (Pierce-Shimomura et al., 2005; Iino and Yoshida, 2009; Izquierdo and Lockery, 2010). Curving rate was calculated as 12.7×NaCl gradient perpendicular to the direction of movement (in millimolars per millimeter) (degrees per second). This transformation was based on a slope of the regression line observed experimentally (Iino and Yoshida, 2009). A stronger perpendicular gradient, such as when the gradient source is lateral to the worm, will result in a larger curving rate. On the other hand, no gradient will result in no curving. This is the case when the source of the gradient is directly in front of or behind the worm.

Environment

Following Iino and Yoshida (2009), the 2D environment is a simulated 4.5mm petri dish containing an NaCl concentration gradient. The concentration (mM) is given by Fick's

equation for two-dimensional diffusion without a border:

$$C = N_o e^{-r^2 400Dt}/4\pi dDt \quad (2)$$

where N_o is the amount of NaCl spotted, D is the diffusion constant of NaCl (0.000015 cm^2/sec), d is the thickness of the plate (0.18 cm), t is time after the spot was administered (sec), and r is the distance from the spot (mm).

The gradient parameters we used were chosen to simulate the chemotaxis assays in Iino and Yoshida (2009). We simulated the worm in the two assays presented there: a grid assay and a radial assay. In the grid assay, there are 12 NaCl spots comprised of an administration of 1 uL, 0.2 M NaCl one hour before the srart of the assay. Model worms begins the assay in the center of a 2 cm square, with an NaCl spot at each corner. The remaining 8 spots are placed 2 cm in the cardinal directions beyond each of the square's spots, forming a cross-like grid. In this configuration, the model worm starts 28.3 mm from the nearest spot. In the radial assay, there is one NaCl spot comprised of two administrations of 5 uL, 0.5 M NaCl: one 19 hours before the start of the assay, and one 4 hours before the start of the assay. In this configuration, the model worm starts 21 mm from the spot. Both assays were performed for a simulated 20 minutes. We did not hold the gradient static, so that over the course of the assay, the chemical gradient continues to diffuse.

Spatial orientation performance metrics

In order to measure how well the model worms orient to the cues in the environment, we adopt the Chemotaxis Index measure used in previous work (Iino and Yoshida, 2009; Soh et al., 2018; Kunitomo et al., 2013), calculated as:

$$\mathrm{CI} = (x - y)/(x + y) \quad (3)$$

where x is the number of observations where the model worm was within a threshold distance of the spot, and y is the number of observations where it was not. Following Iino and Yoshida (2009), we adopt a threshold distance of $\sqrt{2/\pi}$ cm. This threshold was adopted such that in the grid assay worms dispersing without a gradient would obtain a CI of 0. In order to study the dynamics of spatial orientation in more detail, we also considered three additional metrics: the average distance to the nearest NaCl spot over the course of the assay, the minimum distance to a NaCl spot during the assay, and the amount of time it takes for each model worm to reach a NaCl spot (within 1 mm) (for this last metric, model worms that failed to reach the spot are not considered).

Results

In this work, we set out to assess the contributions of each strategy to the overall behavior across different environments. We start by replicating the original grid assay results, then we assess the contribution of each strategy, and finally we analyze the effect of gradient steepness in contributions.

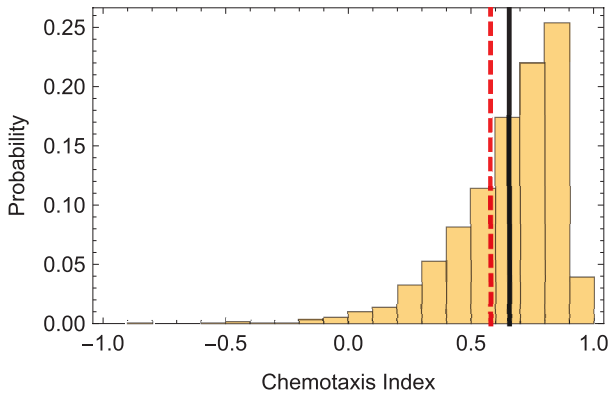

Figure 2: Replicating the original grid assay results. Histogram of the Chemotaxis Index for 5,000 model worms. Solid vertical line represents the mean of the group (0.65). Dashed red line represents the mean observed experimentally in Iino and Yoshida (2009).

Replicating the original grid assay results

As a first step in our analysis of the contribution from the two strategies, we verified that the model worms accurately matched the behavior of the organism. We compared the performance of our model against the empirical data reported in Iino and Yoshida (2009) for the grid assay condition (Fig. 2). They reported a CI of 0.58 (N=67) (dashed red line). When we replicated this experiment for the model worms (N=5,000), we obtained a CI of 0.65 (solid black line), although the variability in the data is wide.

Although the mean of the results reported experimentally and the mean of our simulation are similar, the discrepancies could be due to a number of different reasons. One important factor could be noise. In the previous simulation, there was no noise in the chemical gradient or in the way that it was sensed. In the real worm and in real chemical gradients, noise is likely to be an important factor. As a second step, we analyzed the Chemotaxis Index of the original model worm as implemented in Iino and Yoshida (2009) as a function of noise (blue, Fig. 3). In the original model, the pirouette window is instantaneous. In other words, the model worm calculates the likelihood of a pirouette based on the difference between the chemical concentration in the previous time step of integration and the current one. As can be seen, the performance decays rapidly with noise. In the worm, however, the integration of the chemical concentration in the translational direction is likely to occur over a window of time. In order to study the effect of noise across different windows of concentration integration, we also tested the model worm with a time window of 0.3 (yellow), 0.6 (green), and 1.2 (red) seconds (Fig. 3). This allowed us to examine the combinations of noise and time window of integration that reproduce the mean observed experimentally (dashed line).

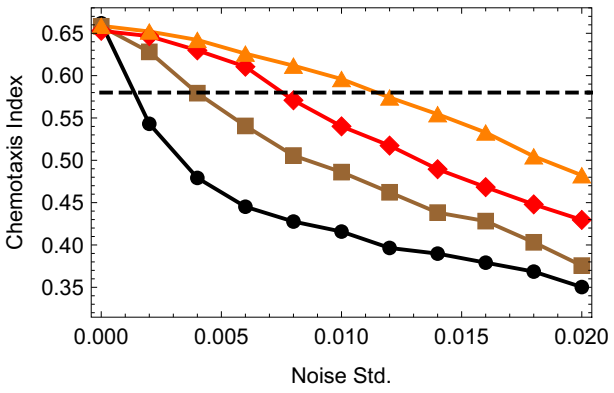

Figure 3: Effect of noise and time window of integration for the pirouette on the Chemotaxis Index. Average chemotaxis index for 5,000 model worms at different levels of noise generated from a Gaussian distribution with standard deviations between 0.0 and 0.02 (x-axis), and across different time windows of sensory integration for the pirouette strategy: 0.1 secs (black); 0.3 secs (brown); 0.6 secs (red); and 1.2 secs (orange). The mean observed experimentally represented by the dashed horizontal line.

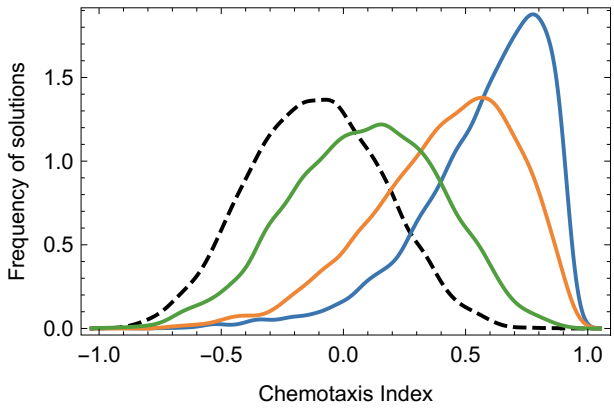

Figure 4: Assessing the contribution from each strategy in the grid assay using the Chemotaxis Index. Smooth histogram of the relative frequency of the Chemotaxis Index obtained by 5,000 model worms on the grid assay for the dual strategy (blue), the klinotaxis-only strategy (orange), the klinokinesis-only strategy (green), and the null strategy (dashed).

Assessing the contribution from each strategy

In order to assess the contributions from each of the strategies to the overall behavior, we examined the four possible combinations that the model worm can adopt based on the presence or absence of each: *dual* strategy, for the model worms with both the strategies in operation; *klinokinesis-only* strategy; *klinotaxis-only* strategy; and the *null* strategy, for the model worms with no orientation strategy, only the default curving bias and baseline pirouette frequency. We first examined the distribution of the resulting Chemotaxis Index during the grid assay for 5,000 model worms on each of the four conditions (Fig. 4). As expected, both strategies contribute to spatial orientation, but klinotaxis seems to contribute more than klinokinesis. Overall, the mean contribution of klinotaxis represents 69.4% of the dual behavior relative to the null behavior; whereas the mean contribution of klinokinesis is 38.4%. Noticeably, the two behaviors are largely complementary, but also redundant given that the addition of the two contributions adds up to over 100% (107.8%).

While the grid assay lends itself well to the Chemotaxis Index, traditionally chemotaxis has been studied more often in plates with a single source in the gradient. The next step in our analysis was to examine each of the four configurations in the radial assay over the course of a simulated 20 minutes (Fig. 5). We examined the performance on the radial assay by measuring the distance to the peak of the gradient over time. As expected, the worms using the dual strategy produced the most effective spatial orientation performance. Also as expected, the worms with no strategy did not find the peak of the gradient, and instead wandered randomly. Of the two populations of worms with the individual strategies, the worms with the klinotaxis-only outperformed those with the klinokinesis-only strategy.

In order to gain a deeper understanding of the performance of each configuration in the radial assay, we measured performance via several measures and plotted the distributions of each (Fig. 6). In addition to the two metrics for assessing general performance: Chemotaxis Index and the average distance to the peak; we also kept track of the time to reach close enough to the peak and the minimum distance to the peak across time. We found that across all measures, the dual strategy was most effective, followed by the klinotaxis-only strategy, and then followed by the klinokinesis-only strategy. The shapes of the dual strategy and klinotaxis-only distributions are quite similar across all four measures, while the shape of the klinokinesis-only distributions tend to be more diffuse, suggesting higher variability. In fact, because the minimum distance metric only takes into account those model worms that reached close enough to the peak, we can see in the minimum distance distributions that many more klinotaxis-only model worms reached the peak than klinokinesis-only model worms. This suggests that the klinotaxis is more reliable than klinokinesis.

Effect of gradient steepness on the contributions

In the majority of experiments in the lab, the steepness profile of the gradient is consistent. However, in the natural world, chemical gradients are likely to span a wide range of shapes and steepness. We would like to better understand how the two strategies contribute in different environments. In order to address this, we consider the effect that the steep-

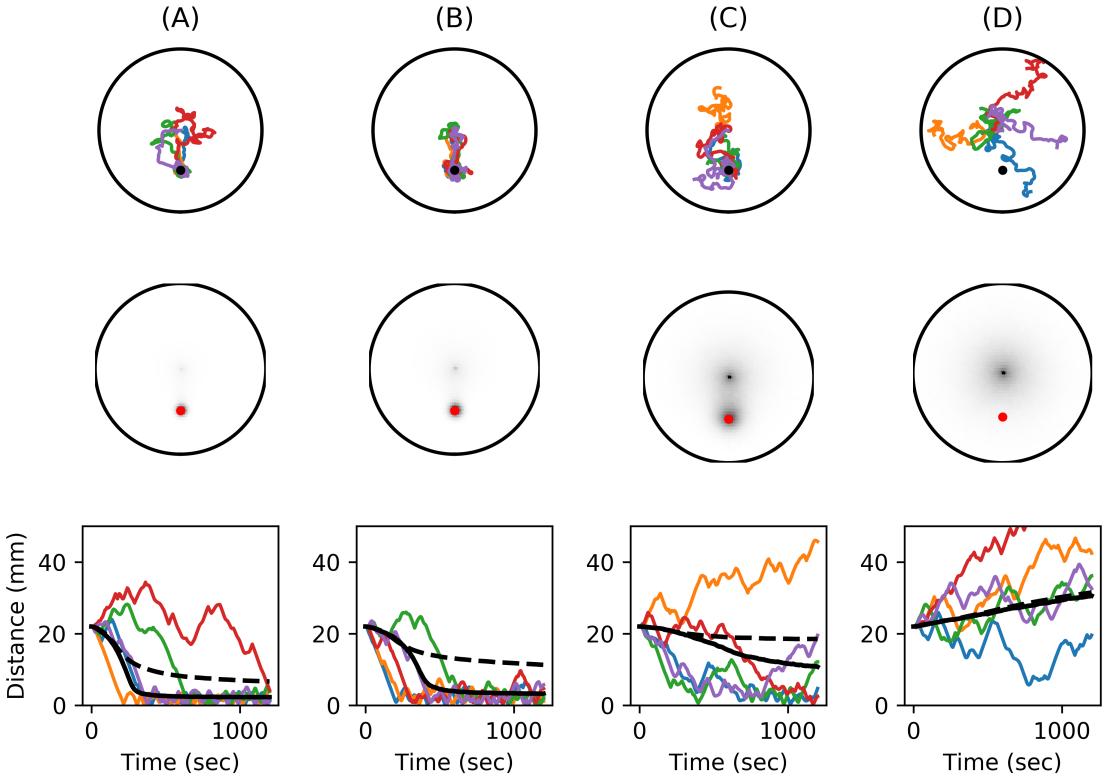

Figure 5: Strategies on the radial assay. The four combinations of strategies we examined are shown in the columns: (A) Dual strategy; (B) Klinotaxis-only strategy; (C) Klinokinesis-only strategy; and (D) Null strategy. Top row depicts a bird's eye view of the traces of the worms over time, for five representative examples. Middle row depicts the density plots for the locations visited using 10,000 worms. Bottom row depicts distance to the peak of the gradient over time for the five model worms in the top row and the median (black) and mean (dashed) of the population from the middle row.

ness of the gradient has on the contribution of each strategy. To address this we designed a steepness experiment, where the concentration gradient was subject to a multiplicative scale parameter, which increased or decreased the gradient's steepness but otherwise left the gradient undistorted. A scale parameter of 1.00 reflects the original gradient. We analyzed the effect of gradient steepness on the contributions of the two strategies in the original grid assay using the Chemotaxis Index (Fig. 7) and in the radial assay using a wider range of metrics (Fig. 8). In both assays, we can see that the effectiveness of the overall spatial orientation behavior improves with the steepness of the gradient (blue traces). In both assays, we can also see that klinotaxis (orange) contributes more than klinokinesis (green) consistently across the full range of the scale considered. Crucially, the overall contribution from klinotaxis becomes relatively a larger portion of the full behavior with steepness. In other words, klinotaxis plays a larger role in steep gradients than in shallow gradients. The opposite is true for klinokinesis, the relative contribution to the overall behavior is larger in the shallow gradients than it is in the steeper gradients.

Effect of noise on the effectiveness

All the work we have shared so far involves concentration gradients that are perfectly smooth and lacking noise. However, this is not the case in the real world - the gradient itself may be noisy and imperfect, or the worm's sensory apparatus may be imperfect. Therefore, we wish to study how noise will affect the model worm's performance. To probe this we applied additive noise to the model worm's sensed concentration, which was sampled from a normal distribution. Additionally, a modification was made to how klinokinesis senses the environment. Previously the sensorimotor transformation was acting on the instantaneous change in the gradient's concentration, but in this experiment the model was parameterized to accommodate time windows of greater length. This implementation takes the average of the differences between the sensed concentrations in the time window. This is consistent with *C. elegans* neuronal trace observations that suggest klinokinesis integrates the difference in concentration sensed over a time window of several seconds (Kato et al., 2014).

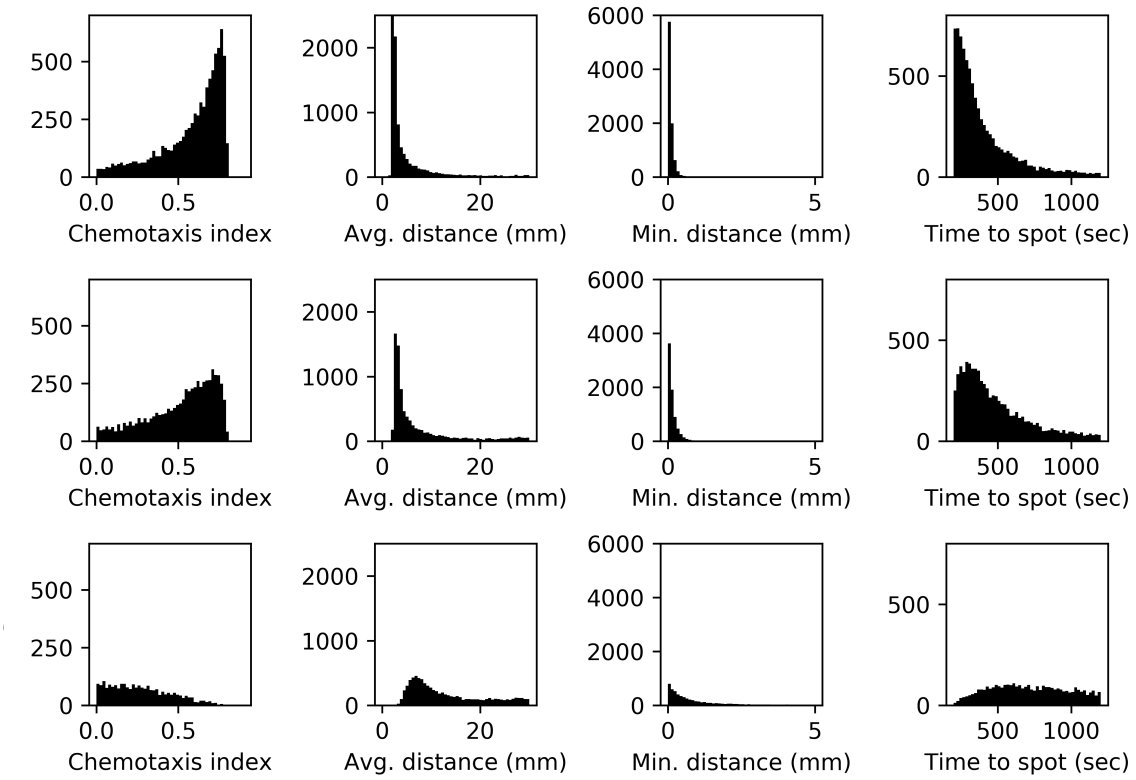

Figure 6: Across all four measures the dual strategy is most effective, followed by klinotaxis-only, then by klinokinesis-only (N=10,000). First row: histograms of dual strategy. Second row: klinotaxis-only. Third row: klinokinesis-only.

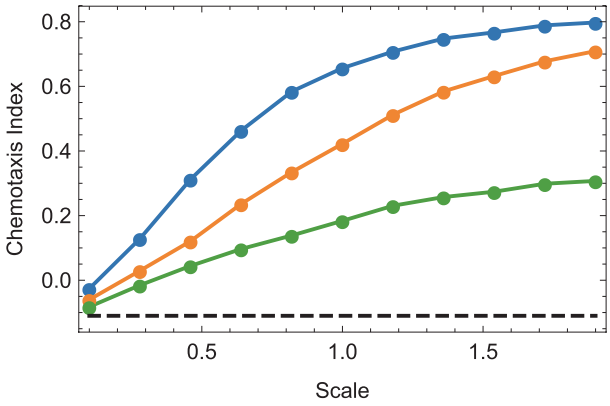

Figure 7: Effect of gradient steepness on the contributions of the two strategies in the grid assay. Depicted are the dual strategy (blue), klinotaxis-only strategy (orange), klinokinesis-only strategy (green), and the null strategy (dashed black).

We found that when relying on an instantaneous pirouette window, the dual strategy degrades quickly in the face of noise (Fig. 9). However, as the length of the pirouette time window increases, so too does its resilience to noise. This increasing resilience largely tapers off after a time window of about a dozen seconds, and we found that for very large time windows (>30 sec), increasing time window size has a *negative* effect on performance.

N-spot experiment

We have investigated environments that are steep, shallow, noisy, or smooth, but they still all have one thing in common: they all contain one NaCl spot. How will the contribution of each strategy change with many NaCl spots? To test this, we selectively disabled spots in the grid assay, creating symmetrical environments of 12, 8, 4, 2, and 1 spot(s). The amount of total NaCl was held constant, such that the spot in the 1-spot environment contained 12 times as much NaCl as the spots in the 12-spot environment. These spots also tend to be steeper than those in the radial assay, as they are allowed to diffuse for only 1 hour before the experiment (versus 4-19 hours in the radial assay).

In the 1-spot condition, all three strategies are at near-chance performance (Fig. 10) probably because the gradient

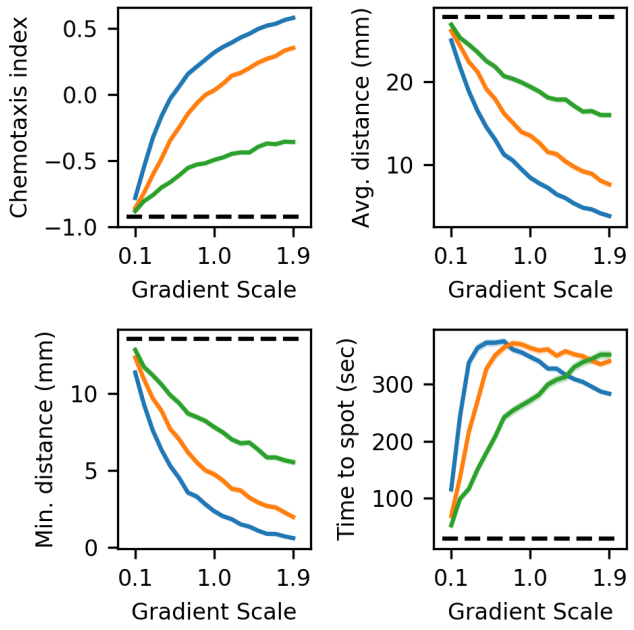

Figure 8: Effect of gradient steepness on the contributions of the two strategies in the radial assay. In shallow environments the strategies perform similarly, while in moderate and steep environments, the klinotaxis strategy makes a greater contribution that the klinokinesis strategy. Depicted are the dual strategy (blue), klinotaxis-only strategy (orange), klinokinesis-only strategy (green), and the null strategy (dashed black). Standard error is show as shaded region.

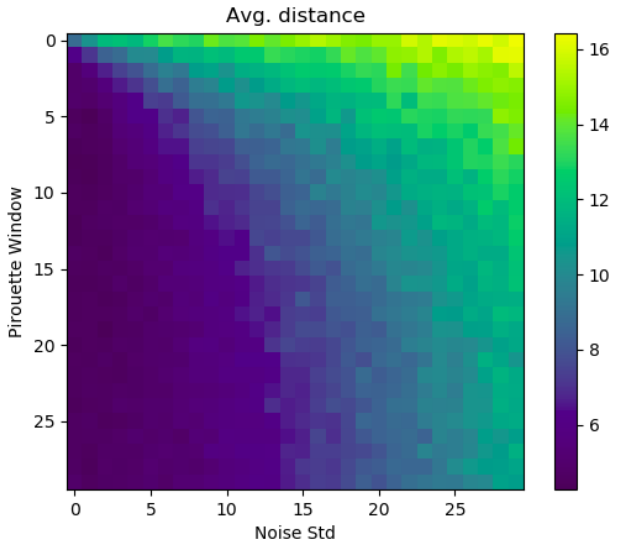

Figure 9: Longer pirouette time windows are more robust in the face of noise, with diminishing returns for windows longer than about 12 seconds. Each cell represents one population of 2,000 model worms.

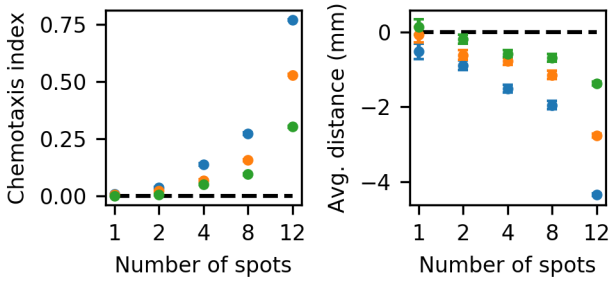

Figure 10: In environments with few spots all three strategies exhibit similar effectiveness, but as the number of spots increases, klinotaxis becomes more important. Depicted are the dual strategy (blue), weathervane strategy (orange), pirouette strategy (green), and no strategy (dashed black). Standard error is show with error bars.

is not well-diffused and many model worms cannot find it. This observation is supported by the fact that there is greater variability in performance in this condition than the others, suggesting that some of the model worms do happen to find the spot and do a good job staying near it. As the number of spots increases, so too does the performance measure of randomly-moving worms because of the change to the geometry of the environment. As a result, it becomes necessary to account for the change to baseline performance, which we did by subtracting the performance of no-strategy model worms from the performance measures of the other strategies. As the number of spots increased, the efficiency of all three strategies did as well, even after subtracting out baseline performance. The efficiency of the klinotaxis-only and klinokinesis only strategies are much more similar in this experiment, only significantly separating in the 12-spot condition. We conclude that the strategies are similarly effective in environments with a low number of spots, but that the importance of klinotaxis increases with the number of spots.

Discussion

We set out to examine the contributions of the klinokinesis and klinotaxis strategy to the overall spatial orientation behavior in the worm across different environments. Our analysis suggests klinotaxis is the primary contributor to chemotaxis in most environments, although klinokinesis always contributes. We found that klinotaxis contributes more in steep gradients and klinokinesis contributes more in shallow gradients.

The two strategies are complementary in terms of timescales and in terms of the bearing between the worm's heading and the source of the gradient. In terms of timescales, klinotaxis operates on a faster timescale than klinokinesis. The time scale of klinotaxis is determined by the

length of lateral head sweeps, whereas klinokinesis operates over the range of the worm's translational movement forward. In terms of spatial scales, klinotaxis contributes the most when the source is perpendicular to the worm's heading, because that produces the largest perpendicular gradient, and it contributes the least when the worm is heading directly towards or away from the source, because the perpendicular gradient is minimal then. Conversely, klinokinesis contributes the most when moving towards or away from the source, and it contributes the least when heading perpendicular to the source. Therefore, despite their difference in effectiveness, the two strategies are more complementary than they are redundant. Ultimately this is the reason that the presence of both strategies operating in parallel lead to better performance than either in isolation.

This work suggests several future experiments and model extensions. First, our investigation into environments with many spots was bound by the desire to design environmental geometries that were continuous with each other, and as such, only a categorical comparison is possible. However, a more fine-grained, continuous analysis could be possible by creating many environments of random layout, save for the number of spots. Additionally, a concept that is lightly explored by the N-spot experiment is the effect of a slightly rugged gradient on chemotaxis performance. However, this concept could be explored independently and in greater depth by using a model of quantifiably rugged landscapes to generate gradients. At present, the model worm evaluates the perpendicular gradient instantaneously. However, the real organism evaluates the perpendicular gradient through lateral head sweeps, meaning that there is a delay between the sensing of dorsal- and ventral-side concentrations. This introduces a temporal dynamic to klinotaxis, and would make possible a systematic study of the interaction between the temporal scales of the two orientation strategies. Finally, at present, the model neglects to include the sinusoidal movement pattern of the real world organism. Implementing this aspect of the organism's movement would would implicitly introduce temporal dynamics into klinotaxis because of the periodicity of the model worm's dorsoventral sweeps - the worm would sense the gradient left one moment, and right the next.

Data availability

The simulation code and data files are publicly available in our research group's GitHub account: github.iu.edu/EASy/DahlbergALife2020.

Acknowledgements

Thank you to Randall Beer for feedback on the model and experiment designs, as well as to Lauren Benson, Marina Dubova, Mahi Luthra, and two anonymous reviewers for their constructive criticism of this manuscript. This material is based upon work supported by the National Science Foundation under Grant No. 1845322.

References

Appleby, P. A. (2014). The role of multiple chemotactic mechanisms in a model of chemotaxis in *C. elegans*: Different mechanisms are specialised for different environments. *Journal of Computational Neuroscience*, 36(3):339–354.

Bretscher, A. J., Kodama-Namba, E., Busch, K. E., Murphy, R. J., Soltesz, Z., Laurent, P., and de Bono, M. (2011). Temperature, oxygen, and salt-sensing neurons in *C. elegans* are carbon dioxide sensors that control avoidance behavior. *Neuron*, 69(6):1099–1113.

Gomez-Marin, A. and Louis, M. (2014). Multilevel control of run orientation in *Drosophila* larval chemotaxis. *Frontiers in Behavioral Neuroscience*, 8(FEB):1–14.

Gray, J. M., Karow, D. S., Lu, H., Chang, A. J., Chang, J. S., Ellis, R. E., Marietta, M. A., and Bargmann, C. I. (2004). Oxygen sensation and social feeding mediated by a *C. elegans* guanylate cyclase homologue. *Nature*, 430(6997):317–322.

Iino, Y. and Yoshida, K. (2009). Parallel use of two behavioral mechanisms for chemotaxis in *Caenorhabditis elegans*. *Journal of Neuroscience*, 29(17):5370–5380.

Izquierdo, E. J. (2019). Role of simulation models in understanding the generation of behavior in *C. elegans*. *Current Opinion in Systems Biology*, 13:93–101.

Izquierdo, E. J. and Lockery, S. R. (2010). Evolution and analysis of minimal neural circuits for klinotaxis in *Caenorhabditis elegans*. *Journal of Neuroscience*, 30(39):12908–12917.

Kato, S., Xu, Y., Cho, C. E., Abbott, L. F., and Bargmann, C. I. (2014). Temporal responses of *C. elegans* chemosensory neurons Are preserved in behavioral dynamics. *Neuron*, 81(3):616–628.

Kunitomo, H., Sato, H., Iwata, R., Satoh, Y., Ohno, H., Yamada, K., and Iino, Y. (2013). Concentration memory-dependent synaptic plasticity of a taste circuit regulates salt concentration chemotaxis in *Caenorhabditis elegans*. *Nature Communications*, 4(May).

Oliveira, S., Rosowski, E., and Huttenlocher, A. (2017). Neutrophil migration in infection and wound repair: going forward in reverse. *Nat Rev Immunol*, 16(6):378–391.

Pierce-Shimomura, J. T., Dores, M., and Lockery, S. R. (2005). Analysis of the effects of turning bias on chemotaxis in *C. elegans*. *Journal of Experimental Biology*, 208(24):4727–4733.

Pierce-Shimomura, J. T., Morse, T. M., and Lockery, S. R. (1999). The Fundamental Role of Pirouettes in *Caenorhabditis elegans*. *Journal of Neuroscience*, 19(21):9557–9569.

Sengupta, P. and Samuel, A. D. (2009). *Caenorhabditis elegans*: a model system for systems neuroscience. *Current Opinion in Neurobiology*, 19(6):637–643.

Soh, Z., Sakamoto, K., Suzuki, M., Iino, Y., and Tsuji, T. (2018). A computational model of internal representations of chemical gradients in environments for chemotaxis of *Caenorhabditis elegans*. *Scientific Reports*, 8(1):1–14.

Varshney, L. R., Chen, B. L., Paniagua, E., Hall, D. H., and Chklovskii, D. B. (2011). Structural properties of the *Caenorhabditis elegans* neuronal network. *PLoS Computational Biology*, 7(2).

White, J. Q., Nicholas, T. J., Gritton, J., Truong, L., Davidson, E. R., and Jorgensen, E. M. (2007). The sensory circuitry for sexual attraction in *C. elegans* males. *Current Biology*, 17(21):1847–1857.

White, S., Southgate, J., Thomson, E., and Brenner, J. (1986). The structure of the nervous system of the nematode *Caenorhabditis elegans*. *Philos Trans R Soc Lond B Biol Sci.*, 314(1165):1–340.